

Relative intensities of $\Delta n = 0$ transitions within the $n = 2$ and $n = 3$ levels in nitrogenlike Ar XII from a θ -pinch plasma

E. Schmieder and H.-J. Kunze

Institut für Experimentalphysik V, Ruhr-Universität, 44780 Bochum, Federal Republic of Germany

(Received 5 October 1994)

In a well diagnosed transient θ -pinch deuterium plasma with a small concentration of argon added, the relative intensities of the $\Delta n = 0$ transitions within the $n = 2$ and $n = 3$ levels were measured at the maximum abundance of the Ar XII ion. The emission spectra of the intrashell transitions were observed in the wavelength range 149–225 Å and 434–784 Å, respectively. Theoretical predictions for electron collision strengths, oscillator strengths, and radiative decay rates were used from the literature to determine the relative intensities which were compared to the experimental results. Therefore, electron collisional excitation rate coefficients and radiative decay probabilities could be indirectly verified. General overall agreement is obtained with a collisional-radiative model which includes 72 levels, although some transitions deviate.

PACS number(s): 52.70.La, 34.80.Kw, 42.55.Vc

In the past 30 years several concepts for x-ray lasers were suggested, and some were realized during the past 10 years. All ideas and results till 1990 are analyzed and discussed in the monograph of Elton [1]. One of the most successful schemes employs Ne-like ions and entails pumping of the $3p$ level through a monopole transition from the ground state $1s^2 2s^2 2p^6$. The dipole excitation rates to the $3s$ and $3d$ levels are comparable, but since the $3p$ level decays only slowly to the $3s$ level, which has a high decay probability to the ground state, population inversion is established between $3s$ and $3p$ resulting in effective short-wavelength laser systems. Cascading from the $3d$ level further increases the inversion; radiation trapping of the $3s$ - $2p$ transition will reduce it.

$3p$ - $3s$ transitions of other isoelectronic sequences with ground state configurations $1s^2 2s^2 2p^k$ ($k = 1$ to 5) have been studied as well, and laser gain has been predicted, for example, for ions of the nitrogen isoelectronic sequence [2,3]. The success of such predictions depends on the reliability of available collisional and radiative rates needed in respective population models, and any experimental confirmation of theoretical data is highly desirable. In a previous publication all $3p$ - $3s$ transitions in neonlike argon were studied and compared with theoretical calculations [4]. We now report investigations on nitrogenlike Ar XII.

Relative intensities of accessible intrashell transitions from $n = 3$ and $n = 2$ levels were studied in a low-density deuterium plasma with an electron density of $2.5 \times 10^{16} \text{ cm}^{-3}$, an electron temperature of about 300 eV, and an argon concentration of the order 1%.

For comparison with observations we set up a collisional-radiative model which included 72 levels and radiative and collisional transitions between them. It is justified to consider a steady-state solution for the population densities of the excited states since their respective time constants are much shorter than that of the variation of the ground state density due to ionization or recombination. Ions in θ -pinch plasma are usually in a transient regime, but the time behavior is readily recorded by observing the time histories of suitable lines

from all ionization stages, and measurements of line intensities are usually carried out at their respective peak emission.

The steady-state population density n_p of the excited levels (p) is calculated by solving a coupled set of equations

$$n_p = \frac{n_e \sum_{q \neq p} n_q X_{qp} + \sum_{q > p} n_q A_{qp}}{\sum_{q < p} A_{pq} + n_e \sum_{q \neq p} X_{pq}} \quad (1)$$

where the A_{pq} are radiative transition probabilities and the X_{pq} are electron collisional rate coefficients, i.e., the product of cross section and electron velocity averaged over the electron velocity distribution function. The assumption of a Maxwellian velocity distribution is well justified for our plasmas. For our model we employed the data given by Bhatia *et al.* [5]; the number of collisional excitation and deexcitation rates was 772. We neglected collisional ionization from the excited states, radiative, dielectronic, and three-body recombination into these states as well as charge transfer processes. Estimates of these processes indicate that their rates are sufficiently smaller [6]. We also calculated the optical thickness for our plasma conditions and found that along the axis of the plasma column it was below 0.4 for the line centers of all our observed transitions. The solution of the radiative transport equation along the axis [7] thus justifies that reabsorption effects may be neglected.

The total population of ion Ar^{11+} was normalized to unity:

$$\sum_{p=1}^{72} n_p = 1. \quad (2)$$

The spectral radiance of each transition was finally calculated by

$$L_{pq} = \frac{h\nu_{pq}}{4\pi} A_{pq} n_p l_p \quad (3)$$

where l_p was the plasma length. In order to check our level population model, we carried out calculations for

the conditions of Bhatia *et al.* [5] and reproduced their results.

Figure 1 shows the experiment arrangement. This is just a brief description of the Bochum reverse field θ pinch; a more detailed description has been previously published in [8]. The current flows through a single-turn aluminum coil with dimensions 21 cm inner diameter, 62 cm length, and 7 cm thick. Inside the pinch coil is a glass discharge tube with inner diameter of 15 cm, which is filled with 19.5 mTorr of deuterium mixed with 1% argon. The plasma is preionized and a bias magnetic field of reverse polarity rises slowly to its peak value of 0.06 T. At this time the main bank is discharged and leads to a stable toroidal plasma column. The main capacitor bank consists of 38 4.5 μ F capacitors connected in parallel and charged up to 35 kV. The current reaches maximum about 5.75 μ s after initiation of the discharge and then is short-circuited by crowbar switches to extend the lifetime of the plasma column. After about 10 μ s elliptical deformation of the plasma column occurs with the onset of an $m = 2$ rotational instability.

Thomson scattering was performed to determine electron density and temperature in the midplane at several radial positions as a function of time and has been reported in Ref. [9]. By varying the concentration of argon from 1% to 5%, it was determined that the 1% concentration did not significantly alter the plasma parameters.

For the spectroscopic measurements of $n = 2$ intrashell transitions (149–225 Å) a 2.2-m grazing incidence VUV monochromator with 1200 grooves/mm high-resolution grating was aligned to view the plasma axially. For the measurements of $n = 3$ intrashell transitions (434–784 Å) a 1.0-m normal incidence VUV monochromator with 2400 grooves/mm grating was aligned to view the plasma axially from the other side. Diaphragms limit the field of view of each monochromator to a 2 cm diameter cross section on the axis in the pinch middle. P-terphenyl scintillators and a photomultiplier were placed at the exit slits to allow the time-resolved observation of the line emission. The branching ratio technique was employed *in situ* to calibrate the variations in sensitivity over the extended spectral range using the data found in the literature [1,10,11]. Thus, the voltage signal from the photomultiplier gave directly the radiance of each line. To monitor the discharge quality of the θ pinch, a 0.25-m visible spectral monochromator was placed to look radially towards the center of the plasma column. The observation of the continuum ensured that all the measurements remained reproducible after repeated discharges. In addition, the $2s^2 2p^3 \ ^2D_{5/2} - 2s^1 2p^4 \ ^2P_{3/2}$ transition at 154.4 Å from Ar XII was monitored as an additional check on the plasma quality, when the $n = 3$

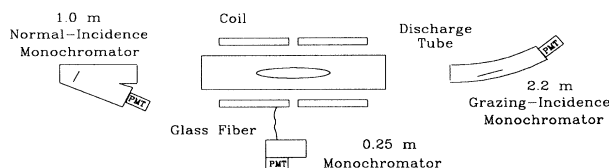


FIG. 1. Experimental layout.

TABLE I. Observed spectral lines of Ar VII–Ar XIII.

Ion	Transition	Wavelength (Å)
Ar VII	$3s^2 \ ^1S_0 - 3s(2S)3p \ ^1P_1$	585.7
	$3s(2S)3p \ ^3P_2 - 3p^2 \ ^3P_2$	637.0
Ar VIII	$2p^6 3s \ ^2S_{1/2} - 2p^6 3p \ ^2P_{1/2}$	713.8
	$2p^6 3s \ ^2S_{1/2} - 2p^6 3p \ ^2P_{3/2}$	700.2
Ar IX	$2p^5 3s \ ^1P_1 - 2p^5 3p \ ^3P_0$	691.2
	$2p^5 3s \ ^3P_1 - 2p^5 3p \ ^3P_2$	589.4
Ar X	$2s^2 2p^5 \ ^2P_{3/2} - 2s2p^6 \ ^2S_{1/2}$	165.5
	$2s^2 2p^5 \ ^2P_{1/2} - 2s2p^6 \ ^2S_{1/2}$	170.6
Ar XI	$2s^2 2p^4 \ ^3P_2 - 2s2p^5 \ ^3P_1$	184.5
	$2s^2 2p^4 \ ^3P_2 - 2s2p^5 \ ^3P_2$	188.8
Ar XII	$2s^2 2p^3 \ ^4S_{3/2} - 2s2p^4 \ ^4P_{3/2}$	218.2
	$2s^2 2p^3 \ ^4S_{3/2} - 2s2p^4 \ ^4P_{5/2}$	224.2
Ar XIII	$2s^2 2p^2 \ ^3P_0 - 2s2p^3 \ ^3S_0$	159.0
	$2s^2 2p^2 \ ^3P_0 - 2s2p^3 \ ^3D_1$	236.2

intrashell transitions were measured. A maximum deviation of 10% was allowed in both cases.

The wavelengths and transitions given in the work were all taken from [12] except for the $3s-3p$ and $3p-3d$ transitions in Ar XII. For these transitions experimental wavelengths are given with an error of about ± 1 Å. LS-coupling notation is used to identify the transitions. Table I identifies the spectral lines that were observed end-on as the plasma went successively through the ionization stages. Their time histories are plotted in Fig 2. At $t = 6.5$ μ s after the initiation of the discharge, Ar XII intensities peaked. The peak spectral radiances of observed lines were averaged over ten discharges and are given in Tables II and III. Table II contains the experimental results for 15 $2s^1 2p^4 \rightarrow 2s^2 2p^3$ transitions. The radiance is normalized to that of the $4P_{5/2} \rightarrow 4S_{3/2}$ transition at 224.2 Å. Table III contains the experimental results for 12 $3p \rightarrow 3s$ and $3d \rightarrow 3p$ transitions. They are normalized to the $4D_{7/2} \rightarrow 4P_{5/2}$ transition at 784.0 Å. This led to a best overall fit to the calculated values. By normalizing the data, any uncertainties of the plasma length and of the argon concentration cancel out. The third column in each table shows the relative theoretical

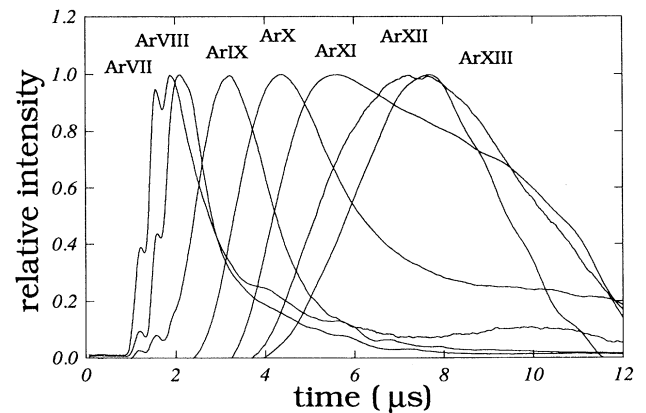


FIG. 2. Time evolution of Ar VII–Ar XIII emission. The maximum of the spectral radiance is normalized to one for each ionization stage.

TABLE II. Relative spectral radiance of $n = 2$ intrashell transitions of Ar XII in the deuterium discharge $n_e = 2.5 \times 10^{16} \text{ cm}^{-3}$ and $kT_e = 300 \text{ eV}$.

λ (Å)	Transition	$I_{\text{theor.}}$	$I_{\text{expt.}}$	$I_{\text{expt.}}/I_{\text{theor.}}$
149.9	$2s^2 2p^3 \ ^2D_{3/2} - 2s^1 2p^4 \ ^2P_{1/2}$	0.38	0.39	1.03
153.6	$2s^2 2p^3 \ ^2D_{3/2} - 2s^1 2p^4 \ ^2P_{3/2}$	0.20	0.20	1.00
154.4	$2s^2 2p^3 \ ^2D_{5/2} - 2s^1 2p^4 \ ^2P_{3/2}$	1.08	1.00	0.92
163.2	$2s^2 2p^3 \ ^2P_{1/2} - 2s^1 2p^4 \ ^2P_{1/2}$	0.06	0.52	8.66
164.5	$2s^2 2p^3 \ ^2P_{3/2} - 2s^1 2p^4 \ ^2P_{1/2}$	0.25	0.70	2.80
167.6	$2s^2 2p^3 \ ^2P_{1/2} - 2s^1 2p^4 \ ^2P_{3/2}$	0.06	0.05	0.83
169.0	$2s^2 2p^3 \ ^2P_{3/2} - 2s^1 2p^4 \ ^2P_{3/2}$	0.15	0.16	1.07
176.6	$2s^2 2p^3 \ ^2P_{1/2} - 2s^1 2p^4 \ ^2S_{1/2}$	0.16	0.15	0.94
178.1	$2s^2 2p^3 \ ^2P_{3/2} - 2s^1 2p^4 \ ^2S_{1/2}$	0.14	0.12	0.86
192.6	$2s^2 2p^3 \ ^2D_{3/2} - 2s^1 2p^4 \ ^2D_{3/2}$	0.68	0.33	0.49
193.6	$2s^2 2p^3 \ ^2D_{5/2} - 2s^1 2p^4 \ ^2D_{5/2}$	0.85	0.15	0.18
215.4	$2s^2 2p^3 \ ^4S_{3/2} - 2s^1 2p^4 \ ^4P_{1/2}$	0.34	0.30	0.88
217.2	$2s^2 2p^3 \ ^2P_{3/2} - 2s^1 2p^4 \ ^2D_{5/2}$	0.14	0.16	1.14
218.2	$2s^2 2p^3 \ ^4S_{3/2} - 2s^1 2p^4 \ ^4P_{3/2}$	0.67	0.69	1.03
224.2	$2s^2 2p^3 \ ^4S_{3/2} - 2s^1 2p^4 \ ^4P_{5/2}$	1.00	1.00	1.00

radiance calculated with our model for our plasma conditions, and the last column gives the ratio of experimental and theoretical values.

With a mean standard deviation of 15% for the $n = 2$ intrashell transitions, the strongly deviating lines given below exempted, a reasonably good agreement between experiment and theory is observed. The deviating transitions are $2s^2 2p^3 \ ^2P_{1/2} - 2s^1 2p^4 \ ^2P_{1/2}$ at 163.2 Å, $2s^2 2p^3 \ ^2P_{3/2} - 2s^1 2p^4 \ ^2P_{1/2}$ at 164.5 Å, $2s^2 2p^3 \ ^2D_{3/2} - 2s^1 2p^4 \ ^2D_{3/2}$ at 192.6 Å, $2s^2 2p^3 \ ^2D_{5/2} - 2s^1 2p^4 \ ^2D_{5/2}$ at 193.6 Å. For the first two transitions the theoretical value seems to be seriously underestimated, and for the last two transitions seriously overestimated. The measured maximum value of each intensity varied by less than 10% from discharge to discharge; the accuracy of the relative sensitivity calibration of the spectrometer was about 10% in the respective spectral range [14]. Some measurements were also reported by Stratton *et al.* [13] on the N -like ions Ti XVI, Cr XVIII, Fe XX, and Ni XXII in a tokamak. Our densities, however, are three orders of magnitude higher.

The mean standard deviation for the $n = 3$ intrashell

transitions is about 30%; again the strongly deviating ones were excluded. This is larger than for the $n = 2$ intrashell transitions because the resolution of the normal incidence monochromator was not sufficient to prevent line overlapping from lower ionization stages and other impurities emissions which were near the Ar XII ion emission (see, for example Fig. 3). Therefore, a deconvolution technique is applied to the measured spectra to determine the correct intensity. To determine the correct intensity of Ar XII emission from the measured signal, the emissions from the earlier Ar ions or other impurities were simply subtracted from the total signal. This technique works quite satisfactory, since the shape of the time history of the ion emission does not change. However, this led to larger uncertainties of the measured intensities of about 20%

The theoretical and experimental relative spectral radiances of $n = 3$ intrashell transitions agree reasonably well for some of the transitions, considering a typical accuracy of 50% in the theoretical line ratios; strong deviations are observed for the transitions $2s^2 2p^2 3s^2 D_{5/2} - 2s^2 2p^2 3p^2 P_{3/2}$ at 538 Å and at 691 Å. For these two

TABLE III. Relative spectral radiance of $n = 3$ intrashell transitions of Ar XII in the deuterium discharge $n_e = 2.5 \times 10^{16} \text{ cm}^{-3}$ and $kT_e = 300 \text{ eV}$.

λ (Å)	Transition	$I_{\text{theor.}}$	$I_{\text{expt.}}$	$I_{\text{expt.}}/I_{\text{theor.}}$
434	$2s^2 2p^2 3s \ ^2P_{3/2} - 2s^2 2p^2 3p \ ^2P_{3/2}$	0.48	0.37	0.77
448	$2s^2 2p^2 3s \ ^2P_{1/2} - 2s^2 2p^2 3p \ ^2D_{3/2}$	0.66	1.21	1.83
451	$2s^2 2p^2 3s \ ^2P_{3/2} - 2s^2 2p^2 3p \ ^2P_{3/2}$	0.18	0.19	1.05
470	$2s^2 2p^2 3s \ ^2P_{3/2} - 2s^2 2p^2 3p \ ^2D_{5/2}$	0.84	0.66	0.79
538	$2s^2 2p^2 3s \ ^2D_{5/2} - 2s^2 2p^2 3p \ ^2P_{3/2}$	0.45	2.07	4.46
542	$2s^2 2p^2 3s \ ^2D_{3/2} - 2s^2 2p^2 3p \ ^2P_{3/2}$	0.41	0.39	0.95
544	$2s^2 2p^2 3s \ ^4P_{3/2} - 2s^2 2p^2 3p \ ^4S_{3/2}$	0.51	0.49	0.96
645	$2s^2 2p^2 3p \ ^2F_{5/2} - 2s^2 2p^2 3d \ ^2G_{7/2}$	1.22	0.68	0.56
691	$2s^2 2p^2 3s \ ^4P_{1/2} - 2s^2 2p^2 3p \ ^4P_{3/2}$	0.22	0.07	0.32
696	$2s^2 2p^2 3s \ ^4P_{1/2} - 2s^2 2p^2 3p \ ^4P_{1/2}$	0.04	0.06	1.50
745	unidentified transition		0.88	
773	$2s^2 2p^2 3s \ ^4P_{1/2} - 2s^2 2p^2 3p \ ^4D_{3/2}$	0.41	0.70	1.71
784	$2s^2 2p^2 3s \ ^4P_{5/2} - 2s^2 2p^2 3p \ ^4D_{7/2}$	1.00	1.00	1.00

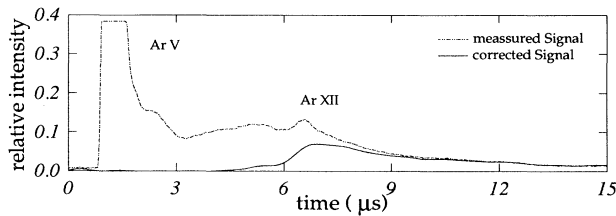


FIG. 3. Normalized time history of the $3s^2P_{3/2} - 3p^2P_{3/2}$ transition.

transitions the measured wavelength and the wavelength derived from calculations using the superstructure code [5] differ by more than 1 Å. An Ar XII transition has been observed at 745 Å which could not be identified.

Blending with Ar XIII is the most probable explanation for the disagreement between experimental and predicted values for the intrashell transitions at 163.2 Å, 164.5 Å, and 538 Å. At 162.96 Å the $2s^22p^2\ ^1D_2 - 2s2p^3\ ^1P_1$ transition has been observed and at 164.82 Å the $2s^22p^2\ ^3P_2 - 2s2p^3\ ^3S_1$ transition has been predicted [12]. Kelly further mentions three unclassified Ar lines at 538.41 Å, 539.19 Å, and 539.79 Å. Also, anomalies have been ob-

served in the time evolution of the $3s^2D_{5/2} - 3p^2P_{3/2}$ emission spectrum at 538 Å. Sporadically, a narrow extremely strong spike with a pulse rise time of about 50 ns would appear superimposed on the signal at approximately the same time of maximum Ar XII abundance. Care was taken not to include these values in the averaged intensity, but this cannot be guaranteed. The cause of the phenomenon is not known.

The discrepancies for the $2s^22p^3\ ^2D_{3/2} - 2s^12p^4\ ^2D_{3/2}$, $2s^22p^3\ ^2D_{5/2} - 2s^12p^4\ ^2D_{5/2}$, and $2s^2p^23s^4P_{1/2} - 2s^22p^23p^4P_{3/2}$ transitions do not appear to be due to the measurements. The theoretical values are much higher than the experimentally observed intensities, and most probably collisional excitation rates are too large.

Future studies should extend the investigations to the lower wavelength region between 25 to 50 Å to cover also transitions from the $3s$, $3p$, and $3d$ levels to the $2s^22p^3$ and $2s2p^4$ levels. It also became obvious that the theoretical wavelengths of $3s-3p$ and $3p-3d$ transitions deviate from the experimental values by up to ± 3 Å. Precise wavelength measurements are definitely needed.

This work was supported by the Deutsche Forschungsgemeinschaft. The authors wish to thank the technical staff of the group for the skillful support.

-
- [1] Raymond C. Elton, *X-Ray Lasers* (Academic Press, San Diego, 1990), p. 102.
 - [2] U. Feldman, J.F. Seely, and A.K. Bhatia, *J. Appl. Phys.* **66**, 2248 (1989).
 - [3] M. Klapisch, M. Cohen, W.H. Goldstein, and U. Feldman, *Radiative Properties of Hot Dense Matter*, edited by W. Goldstein, C. Höoper, J. Gauthier, J. Seely, and R. Lee (World Scientific, Singapore, 1991).
 - [4] N. Preissing, D.O. Campos, H.-J. Kunze, A.L. Osterheld, and R.S. Walling, *Phys. Rev. E* **48**, 2367(1993).
 - [5] A.K. Bhatia, U. Feldman, and J.F. Seely, *At. Data Nucl. Data Tables* **43**, 435 (1989).
 - [6] Hans R. Griem, *Plasma Spectroscopy* (McGraw-Hill, New York, 1964).
 - [7] Allan C.G. Mitchell and Mark W. Zemansky, *Resonance Radiation and Excited Atoms* (Cambridge University Press, London, 1971).
 - [8] R. König, K.-H. Kolk, and H.-J. Kunze, *Phys. Fluids* **30**, 3579 (1987).
 - [9] D.O. Campos and H.-J. Kunze, *Phys. Fluids B* **5**, 1248(1993).
 - [10] M. Mimura, K. Sato, R. Akiyama, and M. Otsuka, *Jpn. J. Appl. Phys.* **29**, 2831 (1990).
 - [11] G.A. Martin and W.L. Wiese, *J. Phys. Chem. Ref. Data* **5**, 537 (1987).
 - [12] R.L. Kelly, *J. Phys. Chem. Ref. Data* **16**, Suppl. No. 1, (1987).
 - [13] B.C. Stratton, H.W. Moos, S. Suckewer, U. Feldman, J.F. Seely, and A.K. Bhatia, *Phys. Rev. A* **31**, 2534 (1985).
 - [14] R. König, K.-H. Kolk, and H.-J. Kunze, *Phys. Scr.* **48**, 9 (1984).